GaSb-Based VCSEL With Buried Tunnel Junction for Emission Around 2.3 μm

Alexander Bachmann, *Student Member, IEEE*, Kaveh Kashani-Shirazi, Shamsul Arafin, and Markus-Christian Amann, *Fellow, IEEE*

***Abstract*—In this paper, we present a device concept and results of an electrically pumped vertical-cavity surface-emitting laser in the (AlGaIn)(AsSb) material system grown on GaSb substrate. The structure consists of an n-doped GaSb/AlAsSb distributed Bragg reflector and a type-I GaInAsSb/AlGaAsSb active region, and incorporates a type-III p^+-GaSb/n^+-InAsSb buried tunnel junction for current as well as optical confinement. Continuous-wave operation up to 75 °C has been achieved at a wavelength of 2.3 μm. The mid-IR emission, the large tunability over a wavelength range of more than 10 nm combined with its single-mode operation makes this device ideally suited for gas-sensing applications.**

***Index Terms*—GaSb, semiconductor lasers, tunable diode laser absorption spectroscopy, vertical-cavity surface-emitting laser (VCSEL).**

I. Introduction

THE DETECTION of hazardous gases for security and environmental purposes has got more and more important within the last years, and a growing demand is observable for gas-sensing systems, creating a booming market. Up to now, mostly systems based on electrochemical sensors have been used. However, they suffer from limited dynamics with long response time and aging issues when used with corrosive gases. Due to its rapid and contactless measurement, detection via tunable diode laser absorption spectroscopy (TDLAS) is a convincing alternative [1]–[3]. In this system, a tunable diode laser source is used in order to scan a wavelength range of several nanometers with a frequency of the order of 10 kHz. The light passes a cell filled with the gas, and a suitable detector measures the intensity of the transmission. If absorption takes place at a specific wavelength, one may easily determine the trace gas species as well as its concentration out of the detected absorption spectrum, since gases show a spectral fingerprint of absorption lines. To be able to measure such a gas with a TDLAS system, a laser source emitting longitudinally as well as transversally in a single mode is needed. Most importantly, this source must be able to scan at least several nanometers without mode hopping at the desired wavelength. Typically, gases show strong absorption lines in the near- to mid-IR wavelength range (800 nm to several micrometers) with increasing line strength at longer wavelengths, which is due to the lower order of harmonics of vibration and rotation oscillations of the molecules. Therefore, one is interested in the development of tunable laser sources emitting in the mid-IR wavelength regime rather than in the near-IR. Particularly between 2 and 3.5 μm, pollutants like CO, CO_2, CH_4, etc., show strong absorption lines that do not or only slightly interfere with water absorption. Besides distributed feedback edge-emitting lasers, vertical-cavity surface-emitting lasers (VCSELs) are the ideally suited laser sources because of their inherent longitudinal single-mode operation, their (electro-) thermal tunability, small beam divergence, low power consumption, and low-cost fabrication due to their on-wafer testing capability. These lasers have already been proved application-suited for WAN applications [4] as well as gas measurements [5]. Just recently, an InP-based VCSEL achieved 2.3 μm emission [6]. However, this seems to be the maximum wavelength feasible with this material system. The materials of choice for covering the mid-IR wavelength range are GaSb-based heterostructures. Impressive results have already been achieved with edge-emitting lasers [7]–[10]. However, only few results have been published on electrically pumped GaSb-based VCSELs, as material properties are partly unknown and processing as well as growth of these materials is still in an initial stage. Baranov *et al.* [11] reported on a device operating under pulsed conditions at 2.2 μm, and a mesa-constricted laser has been presented by Cerutti *et al.* [12] and Ducanchez *et al.* [13].

In this paper, we present a device concept and results of an electrically pumped index-guided VCSEL using a buried tunnel junction (BTJ) as current aperture. The target wavelength for this laser is 2.33 μm in order to cover a strong absorption line of carbon monoxide.

II. Device Structure and Fabrication

The device structure is shown in Fig. 1. The structure is grown by molecular beam epitaxy (MBE) in a Varian GEN II equipped with solid source cells. The whole epitaxy consists of two growth steps. In the first step, a 24-pair, Te-doped lattice-matched AlAsSb/GaSb distributed Bragg reflector (DBR) is grown on a (1 0 0)-orientated, n-doped GaSb substrate. The DBR is followed by an n-doped GaSb current-spreading layer and the active region consisting of five 11-nm-thick $Ga_{0.63}In_{0.37}As_{0.11}Sb_{0.89}$ quantum wells, which are embedded between 8-nm-thick $Al_{0.33}Ga_{0.67}As_{0.03}Sb_{0.97}$ barriers. The wells are compressively strained by 1.6%. The first growth step is completed with a tunnel junction layer,

Manuscript received October 31, 2008; revised December 19, 2008. First published April 24, 2009; current version published June 5, 2009. This work was supported in part by the European Union under the FP6 Project "NEMIS" under Contract FP6-2005-IST-5-031845, in part by the German Federal Ministry of Education and Research under Project "NOSE" under Contract 13N8772, and in part by the Nano Initiative Munich (NIM).

The authors are with the Walter Schottky Institut, Technische Universität München, 85748 Garching, Germany (e-mail: bachmann@wsi.tum.de; kashani@wsi.tum.de; arafin@wsi.tum.de; amann@wsi.tum.de).

Color versions of one or more of the figures in this paper are available online at http://ieeexplore.ieee.org.

Digital Object Identifier 10.1109/JSTQE.2009.2013361

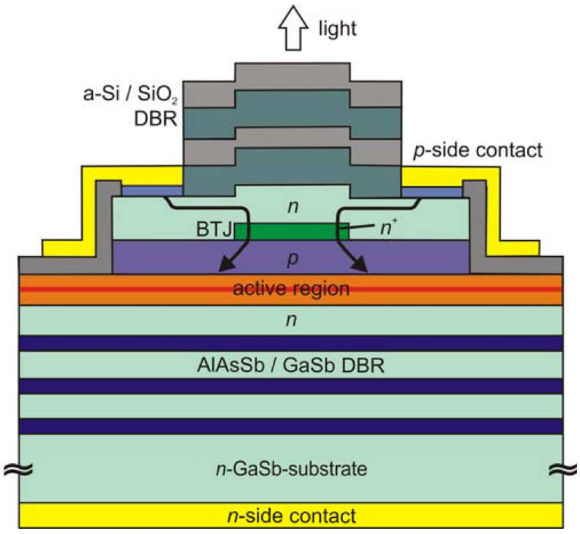

Fig. 1. GaSb-based VCSEL structure with BTJ. The BTJ serves as current aperture, as depicted by the arrows. The structure is composed of two DBRs, one epitaxially grown on the substrate and one consisting of dielectrics on top. The active region is placed between the AlAsSb/GaSb mirror and the BTJ.

made of highly p-doped GaSb (p doping of 2×10^{19} cm^{-3}) and n-doped $\mathrm{InAs}_{0.91}\mathrm{Sb}_{0.09}$.

For the fabrication of an intracavity contact, circular as well as elliptical mesas are defined by standard UV lithography and subsequent dry chemically etching of the InAsSb layer. For the following second growth step, a special atomic hydrogen cleaning procedure is necessary in order to remove oxides as well as carbon contaminations from the surface [14]. This step is performed *in situ* directly before the second epitaxy. Next, an n-doped GaSb-layer and highly Te-doped InAsSb contact layer [15] are grown. In order to achieve a low resistive lateral current flow from the p-side contact to the tunnel junction at the center of the final device, a thickness of approximately 1 μm is chosen for the regrown GaSb layer.

The processing of the device begins with the formation of the VCSEL mesa by reactive ion etching with Cl_2. In the next step, the device is passivated with a 200-nm-thick sputtered SiO_2 layer. After the removal of this layer as well as the contact layer at the upper laser facet, the top and backside metal contacts on the substrate are deposited. By Ar-etching and Ti/Pt/Au sputtering, a low resistive ($\rho = 5 \times 10^{-6}$ $\Omega{\cdot}\mathrm{cm}^2$) metal–semiconductor top contact can be realized without annealing, as further explained in [15]. The backside Ti/Pt/Au contact is directly deposited on the substrate, leading to a low resistive contact due to the large contact area. Finally, by e-beam evaporation, a four-pair amorphous $\mathrm{Si}/\mathrm{SiO}_2$ dielectric DBR is deposited and structured by a liftoff technique.

III. Optical Design

A. Distributed Bragg Reflectors

As the gain length in a VCSEL is of the order of only several nanometers, it is clear that highly reflective mirrors with $R > 99.5\%$ are needed. This requirement is fulfilled with distributed Bragg reflectors, composed of quarterwave layer stacks with alternating layers of high- and low-refractive index.

In the GaSb-based VCSEL design described in this paper, a 24-pair n-doped epitaxial bottom DBR consisting of $\mathrm{AlAs}_{0.09}\mathrm{Sb}_{0.91}$ and GaSb is used. This material combination offers a refractive index difference of $\Delta n \approx 0.7$, making it excellently suited for highly reflective DBRs with a low number of layer pairs. However, due to the average doping of 5×10^{17} cm^{-3}, free carrier absorption [16] takes place, limiting the achievable peak reflectivity of the mirror to 99.8%. As this reflectivity is limited by absorption, it cannot be further enhanced by additional layer pairs.

For the upper DBR, a dielectric mirror, formed by e-beam evaporation, has been chosen. As the growth is interrupted in order to structure the BTJ mesas, an upper epitaxial DBR would have to be grown in the second MBE step. However, the optical properties of the layers that are not grown on epi-ready wafers are insufficient. Second, the high temperature needed during the growth of AlAsSb would produce a hardly controllable blueshift of the active region emission (further treated in Section V). These problems are avoided by using the dielectric DBR, which is made of four pairs of amorphous Si and SiO_2 with a high refractive index contrast of $\Delta n \approx 1.9$. Both materials offer low optical absorption at wavelengths >2 μm [17]. The peak reflectivity is calculated to be 99.7%.

B. Cavity Design

While designing the cavity, one has to ensure that the active region is placed in an antinode of the field in order to achieve the maximum field overlap with the active region. The highly doped, and therefore, strongly absorbing BTJ has to be placed in a node to reduce the optical absorption as much as possible. Furthermore, one has to add current spreading layers for the lateral current flow, as further treated in Section IV. The tradeoff between a short optical thickness of the cavity for low absorption losses and low electrical resistance led to a 3λ-thick cavity. The field distribution in the different layers is shown in Fig. 2. One current spreading layer is placed between the epitaxial DBR and the active region. In order to achieve a low resistive lateral current flow, three spreading layers are needed between the BTJ and the dielectric DBR. The BTJ is placed in the neighboring node to the active region.

By structuring the BTJ and overgrowing it without any surface planarizing technique, the cavity length changes from the etched to the nonetched regions. Therefore, the effective index decreases outside the tunnel junction [18]. For technological reasons, the BTJ etch depth in the present device is comparatively high at 72 nm, yielding a $\Delta n_{\mathrm{eff}} \approx 0.1$. Therefore, strong lateral optical confinement takes place in this VCSEL.

IV. Electrical Design

A. Buried Tunnel Junction

A major challenge in achieving continuous-wave (cw) operation with good spectral properties is the realization of an electrical current aperture. Oxide apertures have not yet been

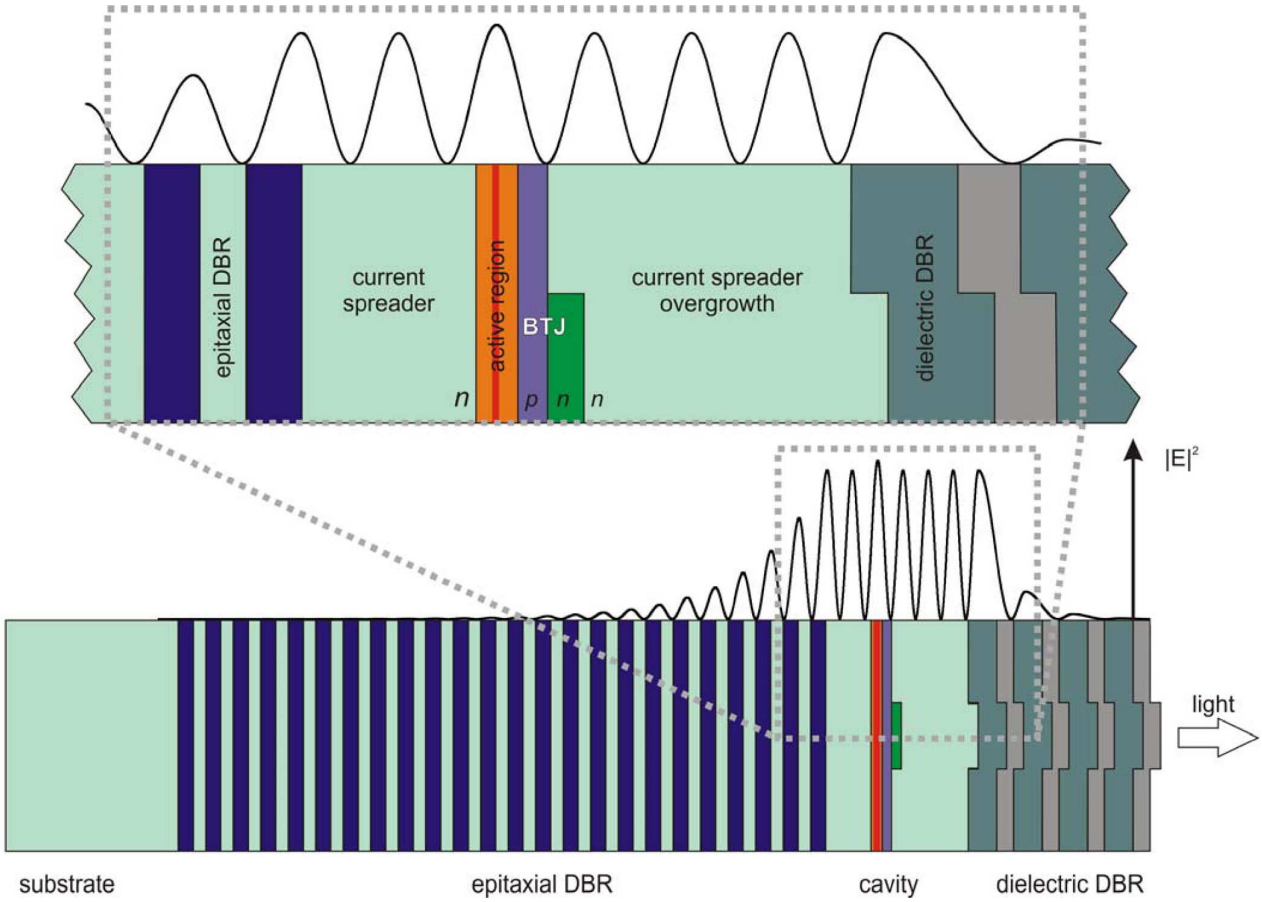

Fig. 2. Field distribution in GaSb-based BTJ-VCSEL. The active region is placed in an antinode of the field, whereas the BTJ is in a node.

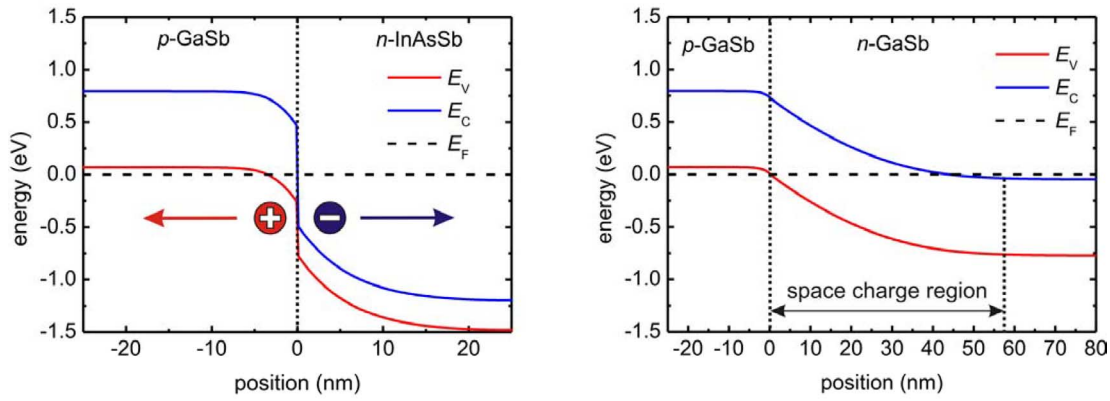

Fig. 3. (a) Band diagram of the tunnel junction, i.e., the p-GaSb:Si/n-InAsSb:Si layer structure with an n- and p-doping of 2×10^{19} cm^{-3}. A broken-gap type-III heterojunction is formed, leading to a highly conductive intracavity contact. (b) The blocking pn-junction formed at the etched surfaces. Due to the large space charge region, a highly resistive contact arises, creating efficient current confinement to the BTJ region. E_{V} and E_{C} are the valence and conduction band edge energies, respectively, and E_{F} the Fermi energy.

realized in GaSb-based VCSELs with sufficient blocking capabilities [19]. In the BTJ-VCSEL, a BTJ is used, made of a type-III heterojunction of p-doped GaSb and n-doped InAsSb. Both layers are doped with Si, being an amphoteric dopant. Besides the easy growth, this dopant has the big advantage of being immobile in the lattice, while a Be/Te doping of GaSb and InAsSb, respectively, features diffusion problems [20], leading to aging issues. The band structure of the heterojunction is shown in Fig. 3(a). Due to the type-III alignment, a relatively low doping of only 2×10^{19} cm^{-3} in both BTJ layers can be used in order to achieve intracavity contacts with a specific resistance as low as 2.5×10^{-6} Ω·cm^2 [21], [22]. Due to the etching of the InAsSb layer at the outer parts of the VCSEL structure and the subsequent overgrowth by n-GaSb (n doping of 5×10^{17} cm^{-3}), a

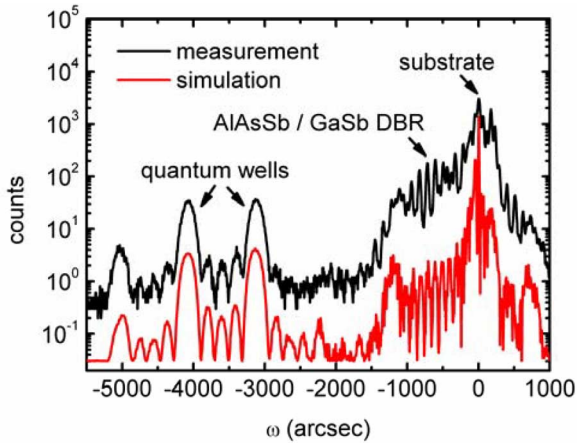

Fig. 4. X-ray diffractometry measurement of "half" 2.3 μm VCSEL after the first growth step. The peaks from the DBR layers and quantum wells can be clearly identified, showing good agreement with the simulation. The Pendelloesung fringes between the main peaks of the quantum well signal prove the good material quality.

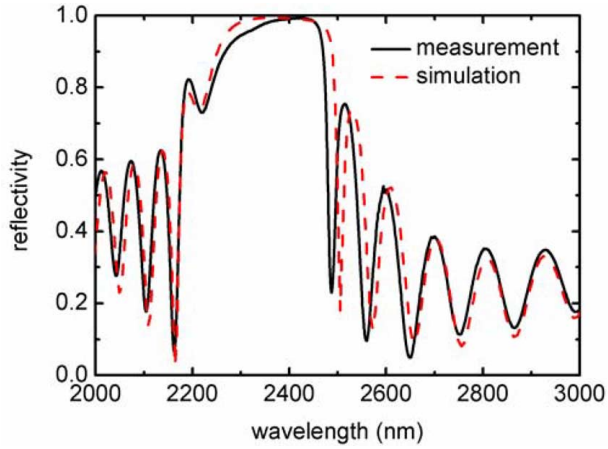

Fig. 5. Reflectivity spectrum of "half" 2.3 μm VCSEL after the first growth step with a stop band center wavelength of 2.31 μm. The dip is caused by the cavity between the epitaxial DBR and the semiconductor–air interface. The simulation shows a good agreement.

highly blocking, reversely biased p^+n-junction is formed outside the BTJ [see Fig. 3(b)]. On test samples, a blocking ratio, defined as the current density flowing through the conductive part divided by the current density at the outer etched surfaces, as high as 2×10^4 has been achieved after atomic hydrogen cleaning (see Section II). In the VCSEL, this results in an effective current confinement to the center of the device, i.e., the BTJ area. Current is injected through the ring contact around the dielectric DBR in the GaSb current spreader. It converges to the tunnel junction aperture and restricts the pumped area of the active region to the diameter of the BTJ mesa plus an additional approximate 2 μm radial diffusion of carriers.

B. Epitaxial DBR

As described in Section III, a major advantage of the AlAsSb/GaSb material combination against, e.g., DBRs based on InP, is its high refractive index contrast. However, from the electrical point of view, there is a strong disadvantage resulting from the high heterointerface resistance of 3.63×10^{-5} $\Omega{\cdot}\mathrm{cm}^2$ per interface at a current density of 1 $\mathrm{kA}{\cdot}\mathrm{cm}^{-2}$ due to large space charge regions. As previously shown in [23], the resistance can be strongly reduced by using interface modifications, such as a 10-period AlSb/GaSb short-period superlattice. Moreover, with an increased doping of 2×10^{18} cm^{-3} and 1×10^{18} cm^{-3} at the interface layers in the field minimum and the field maximum, respectively, the resistance can be reduced to 1.43×10^{-5} $\Omega{\cdot}\mathrm{cm}^2$. The doping of the bulk layers has been chosen after a tradeoff between electrical conductivity and low absorption losses to a concentration of 5×10^{17} cm^{-3}.

V. Results

The research described in this paper aimed on the fabrication of VCSELs emitting around 2.3 μm for the detection of carbon monoxide by TDLAS. Devices were fabricated as described in Section II. Fig. 4 shows an X-ray diffractometry measurement of a "half" VCSEL device after the first growth step. Besides the substrate peak, the peaks arising from the epitaxial mirror layers and the signal of the quantum wells of the active region can clearly be seen. The Pendelloesung fringes between the main peaks of the quantum well signal prove the good material quality of the active material.

The reflection measurement in Fig. 5 shows the reflectivity spectrum after the first growth step, i.e., the structure consisting of the epitaxial DBR and "half" the cavity, including active region and BTJ. The broad dip at 2218 nm is due to the cavity between the DBR and the ≈33% reflection at the semiconductor–air interface. The reason for the apparent misalignment of the cavity dip is the incomplete cavity. As can be confirmed by simulation, the dip is at the correct position.

For the design of the active region, a commonly known blueshift of the emission from the quantum well material GaInAsSb has to be taken into account. As previously described in [24], a blueshift of up to 61 meV occurs when annealing the material at a temperature exceeding 430 °C. For the oxide desorption before the second growth step, the structure is exposed to a temperature of 580 °C and the substrate temperature during overgrowth is about 530 °C for approximately 2 h. This results in the mentioned blueshift, which cannot be avoided. However, it can be compensated by growing QW layers with a higher In content to reach the target emission wavelength after annealing. As can be seen in Fig. 6, the photoluminescence of a test sample with the VCSEL's active region at 15 K shows a blueshift of 60 meV.

The manufactured devices were tested on a temperature-controlled copper stage with an ILX Lightwave LDP-3811 current source. Light–current (*L–I*) characteristics were measured with a Peltier-cooled extended InGaAs detector. Fig. 7 shows the *L–I–V* characteristics of a device with a circular aperture diameter of 8 μm. CW operation has been obtained up to a temperature of 75 °C. Low threshold currents of 1.35 mA at – 10 °C have been achieved, corresponding to an effective threshold current density of 1.2 $\mathrm{kA}{\cdot}\mathrm{cm}^{-2}$ assuming a 2 μm diffusion length

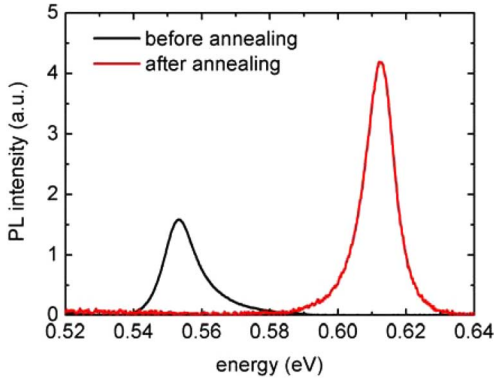

Fig. 6. Photoluminescence spectra of active region test samples at 15 K. After annealing at 580 °C, a blueshift as well as an increase in intensity is observed.

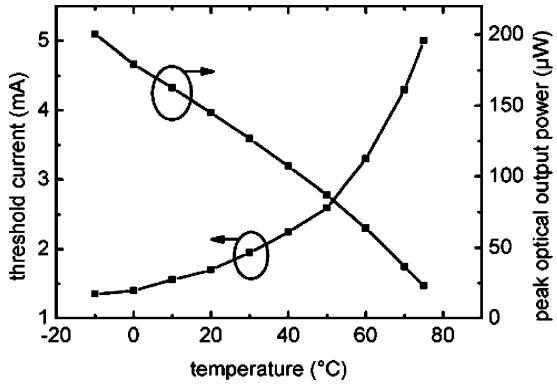

Fig. 8. Temperature-dependent threshold current and peak optical output power of 8-μm aperture BTJ-VCSEL.

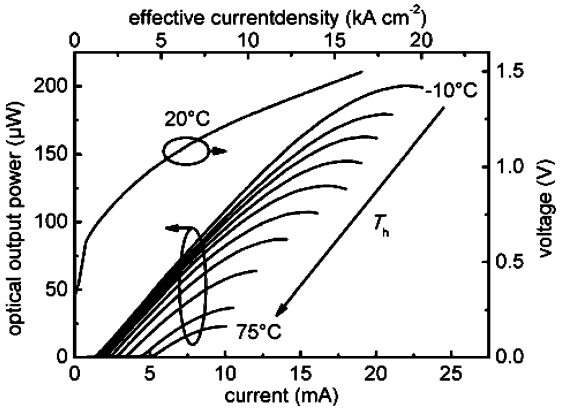

Fig. 7. CW *L–I–V* characteristics of GaSb-based BTJ-VCSEL with a circular aperture diameter of 8 μm.

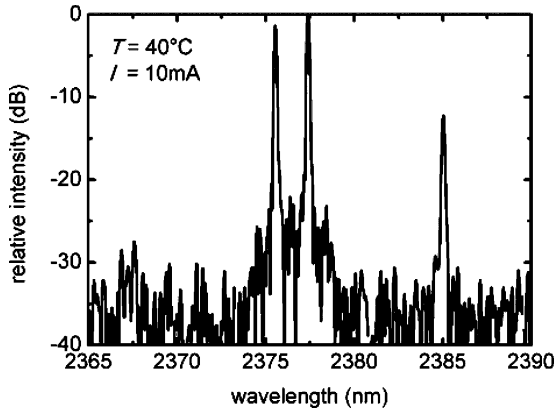

Fig. 9. Multimode spectrum of GaSb-based BTJ-VCSEL with a circular aperture diameter of 8 μm.

of carriers in the active region (as simulated, without considering the diffusion length, the upper limit for the threshold current density is 2.7 kA·cm^{-2}). The lasing threshold voltage is 0.75 V, showing that some series resistance is present in the device, probably resulting from the DBR and the metal–semiconductor contact. The differential resistance is smaller than 100 Ω above threshold. In the investigated temperature range (– 10 °C to 75 °C), the threshold current increases and the output power decreases with increasing temperature (see Fig. 8). This may be caused by a misaligned cavity mode and gain maximum or by the strongly increasing nonradiative Auger processes at higher temperatures.

The investigated device shows multimode emission at wavelengths between 2.375 and 2.385 μm at 40 °C and a current of 10 mA. By increasing the temperature from – 10 °C to 50 °C at a constant bias of 10 mA, the VCSEL emission (see Fig. 9) is tunable over a range from 2.367 to 2.382 μm for the strongest mode, corresponding to a tunability of 0.22 nm/K. By electrothermal tuning, one achieves a tunability range of 10 nm or 0.59 nm/mA (at – 10 °C).

However, for TDLAS applications, single-mode emission is favorable, which has been achieved with a side-mode suppression ratio of 20 dB by using an elliptical aperture diameter of 3.1 and 5.2 μm semiminor and semimajor axes, respectively. This device features a threshold current of 2.3 mA and a maximum output power of 80 μW at – 10 °C and similar temperature-dependent threshold characteristics mentioned earlier; however, the maximum temperature is limited to 50 °C. Temperature-dependent spectra of this device are presented in Fig. 10. The tunability again shows a linear dependence on temperature with a slope of 0.22 nm/K (see Fig. 11). Several current-dependent spectra are shown in Fig. 12. At room temperature, the device can be tuned over 8 nm, corresponding to 0.61 nm/mA (Fig. 13). Due to this large tunability, a large number of gas absorption lines can be addressed. The side-mode suppression ratio always is $\geq$20 dB.

By using the (electro-) thermal tunability rates $\partial\lambda/\partial P$ and $\partial\lambda/\partial T$, where P denotes the total electrical power, one is able to estimate the thermal resistance $R_{\rm th}$ of the devices with

$$R_{\rm th} = \frac{\partial T}{\partial P} = \frac{\partial\lambda/\partial P}{\partial\lambda/\partial T}. \quad (1)$$

By considering the applied voltage, one may calculate the applied power tunability to 0.395 nm/mW, yielding a thermal resistance of 1800 K/W. This value is better than expected, showing the good thermal properties of the material, especially the DBR. With the calculated value, the elevated temperature in the active region can be estimated to about 4 K at threshold and 40 K at rollover (total electrical power at room temperature).

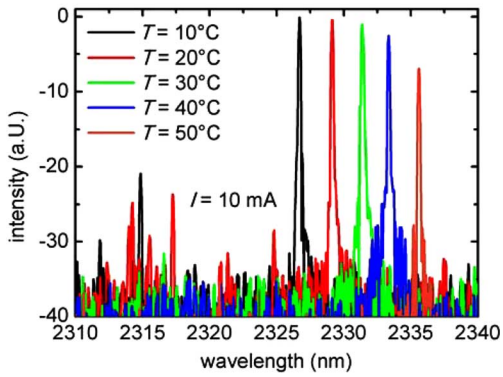

Fig. 10. Temperature-dependent single-mode spectra (SMSR $\geq$ 20dB) of GaSb-based BTJ-VCSEL with elliptical aperture diameters of 6.2 and 10.4 μm at a constant bias of 10 mA.

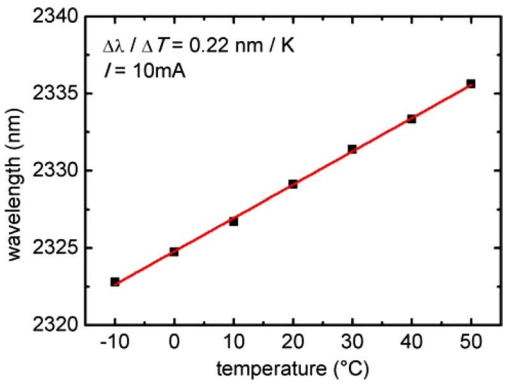

Fig. 11. Temperature tunability of GaSb-VCSEL from Fig. 10.

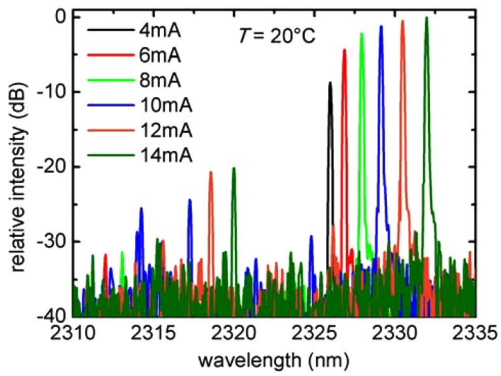

Fig. 12. Current-dependent single-mode spectra (SMSR $\geq$ 20dB) of GaSb-based BTJ-VCSEL with elliptical aperture diameters of 6.2 and 10.4 μm at 20 °C.

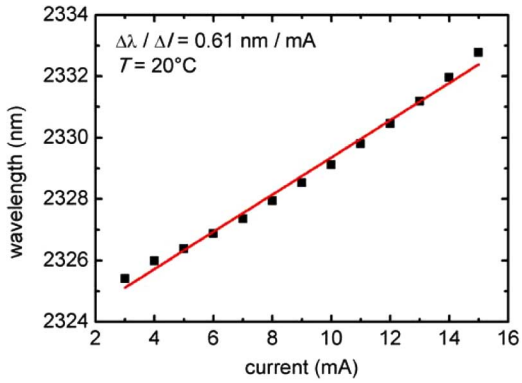

Fig. 13. Current tunability of GaSb-VCSEL from Fig. 12.

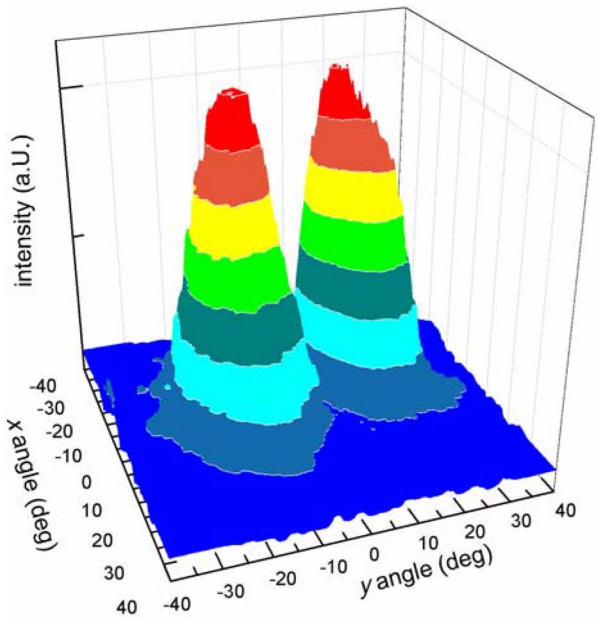

Fig. 14. Far-field measurement of GaSb-based BTJ-VCSEL with 6-μm aperture diameter, yielding the LP11 mode.

On a VCSEL with 6-μm circular aperture diameter showing also single-frequency behavior, far-field measurements have been performed. Fig. 14 shows the measured far field, yielding the LP11 mode. The fundamental LP01 mode could not be seen. The reason for the single higher order mode emission of the VCSEL seems to be the strong optical confinement of the VCSEL, leading to very large transversal mode spacing. Calculated values are in the range of 10 nm. Due to this, a slightly false cavity length leads to the preference of a higher mode, which then shows the higher DBR reflectivity, and therefore, the stronger amplification than the fundamental mode.

The reason for the low output power of only 200 and 80 μW at -10 °C for the presented circular and elliptical aperture devices, respectively, and also the low differential efficiencies of approximately 2% are currently under investigation. Besides the above-mentioned possible misaligned cavity mode and gain maximum, several reasons are likely explanations: Due to an insufficient knowledge of material data, the active region and highly absorbing tunnel junction layers may not be situated exactly in the (anti-)node of the field, leading to improvable device performance. Furthermore, high diffraction losses due to the LP11 mode and also optical absorption in the doped epitaxial mirror as well as the cavity may degrade the device properties. The output power also may be increased by decreasing the top mirror reflectivity. Finally, an optimized active region concerning band offsets, barrier thickness, and number of quantum wells may increase both output power as well as efficiency [25].

VI. Conclusion and Outlook

In this paper, a device concept and first results for a GaSb-based VCSEL with BTJ have been presented. The concept incorporates an epitaxial mirror grown on a GaSb substrate, a five-quantum-well active region, and a dielectric Bragg mirror for light output. The index guiding associated with the BTJ technology allows single-mode operation with the LP11 transversal mode. CW operation at wavelengths between 2.3 and 2.4 μm has been achieved up to a temperature of 75 °C, with low threshold currents of only 1.35 mA at – 10 °C. Due to their high tunability rates of 0.22 nm/K and more than 0.6 nm/mA, the devices are very well suited for gas-sensing applications with TDLAS.

This device concept may easily be applied to GaSb-based lasers emitting in the entire 2–3 μm wavelength range. Application-suited devices are expected by achieving higher output power and fundamental mode emission with the above-mentioned optimizations.

Acknowledgment

The authors thank the measurement support by VERTILAS GmbH.

References

[1] A. Vicet, D. A. Yarekha, A. Pérona, Y. Rouillard, S. Gaillard, and A. N. Baranov, "Trace gas detection with antimonide-based quantum-well diode lasers," *Spectrochim. Acta, A*, vol. 58, pp. 2405–2412, 2002.

[2] P. Werle, F. Slemr, K. Maurer, R. Kormann, R. Mücke, and B. Jänker, "Near- and mid-infrared laser-optical sensors for gas analysis," *Opt. Lasers Eng.*, vol. 37, pp. 101–114, 2002.

[3] P. Werle, "A review of recent advances in semiconductor laser based gas monitors," *Spectrochim. Acta, A*, vol. 54, pp. 197–236, 1998.

[4] C. Chang-Hasnain, "Tunable VCSEL," *IEEE J. Sel. Topics Quantum Electron.*, vol. 6, no. 6, pp. 978–987, Nov./Dec. 2000.

[5] V. Weldon, J. O'Gorman, J. J. Pérez-Camacho, D. McDonald, J. Hegarty, J. C. Conolly, N. A. Morris, R. U. Martinelli, and J. H. Abeles, "Laser diode based oxygen sensing: A comparison of VCSEL and DFB laser diodes emitting in the 762 nm region," *Infrared Phys. Technol.*, vol. 38, pp. 325–329, 1997.

[6] M. Ortsiefer, G. Böhm, M. Grau, K. Windhorn, E. Rönneberg, J. Rosskopf, R. Shau, O. Dier, and M.-C. Amann, "Electrically pumped room temperature CW VCSELs with 2.3 μm emission wavelength," *Electron. Lett.*, vol. 42, no. 11, pp. 640–641, 2006.

[7] M. Grau, C. Lin, O. Dier, C. Lauer, and M.-C. Amann, "Room-temperature operation of 3.26 μm GaSb-based type-I lasers with quinternary AlGaInAsSb barriers," *Appl. Phys. Lett.*, vol. 87, no. 24, pp. 241104-1–241104-3, 2005.

[8] C. Lin, M. Grau, O. Dier, and M.-C. Amann, "Low threshold room-temperature continuous-wave operation of 2.24–3.04 μm GaInAsSb/AlGaAsSb quantum-well lasers," *Appl. Phys. Lett.*, vol. 84, no. 25, pp. 5088–5090, 2004.

[9] J. G. Kim, L. Shterengas, R. U. Martinelli, and G. L. Belenky, "High-power room-temperature contiunuous wave operation of 2.7 and 2.8 μm In(Al)GaAsSb/GaSb diode lasers," *Appl. Phys. Lett.*, vol. 83, no. 10, pp. 1926–1928, 2003.

[10] T. Lehnhardt, M. Hümmer, K. Rößner, M. Müller, S. Höfling, and A. Forchel, "Continuous wave single mode operation of GaInAsSb/GaSb quantum well lasers emitting beyond 3 μm," *Appl. Phys. Lett.*, vol. 92, no. 18, pp. 183508-1–183508-3, 2008.

[11] A. N. Baranov, Y. Rouillard, G. Boissier, P. Grech, S. Gaillard, and C. Alibert, "Sb-based monolithic VCSEL operating near 2.2 μm at room temperature," *Electron. Lett.*, vol. 34, no. 3, pp. 281–282, 1998.

[12] L. Cerutti, A. Ducanchez, P. Grech, A. Garnache, and F. Genty, "Room-temperature, monolithic, electrically-pumped type-L quantum-well Sb-based VCSELs emitting at 2.3 μm," *Electron. Lett.*, vol. 44, no. 3, pp. 203–205, 2008.

[13] A. Ducanchez, L. Cerutti, P. Grech, and F. Genty, "Room-temperature continuous-wave operation of 2.3-μm Sb-based electrically pumped monolithic vertical-cavity lasers," *IEEE Photon. Technol. Lett.*, vol. 20, no. 20, pp. 1745–1747, Oct. 2008.

[14] G. R. Bell, N. S. Kaijaks, R. J. Dixon, and C. F. McConville, "Atomic hydrogen cleaning of polar III–V semiconductor surfaces," *Surf. Sci.*, vol. 401, pp. 125–137, 1998.

[15] C. Lauer, O. Dier, and M.-C. Amann, "Low-resistive metal/n^+-InAsSb/n-GaSb contacts," *Semicond. Sci. Technol.*, vol. 21, pp. 1274–1277, 2006.

[16] R. A. Soref and J. P. Lorenzo, "All-silicon active and passive guided-wave components for 1.3 and 1.6 μm," *IEEE J. Quantum Electron.*, vol. QE-22, no. 6, pp. 873–879, Jun. 1986.

[17] E. D. Palik, *Handbook of Optical Constants of Solids*. Washington, DC: Academic, 1985.

[18] G. R. Hadley, "Effective index model for vertical-cavity surface-emitting lasers," *Opt. Lett.*, vol. 20, no. 13, pp. 1483–1485, 1995.

[19] A. Salesse, R. Hanfoug, Y. Rouillard, F. Genty, G. Almuneau, L. Chusseau, A. Baranov, C. Alibert, J. Kieffer, E. Lebeau, and J. M. Luck, "Wet oxidation of AlAsSb alloys catalyzed by methanol," *Appl. Surf. Sci.*, vol. 161, pp. 426–433, 2000.

[20] O. Dier, M. Grau, C. Lauer, C. Lin, and M.-C. Amann, "Diffusion of dopants in highly (10^{20} cm^{-3}) n- and p-doped GaSb-based materials," *J. Vac. Sci. Technol. B, Microelectron. Nanometer Struct.*, vol. 23, no. 2, pp. 349–53, 2005.

[21] O. Dier, M. Sterkel, M. Grau, C. Lin, C. Lauer, and M.-C. Amann, "Tunnel junctions for ohmic intra-device contacts on GaSb-substrates," *Appl. Phys. Lett.*, vol. 85, no. 12, pp. 2388–2389, 2004.

[22] O. Dier, C. Lauer, and M.-C. Amann, "n-InAsSb/p-GaSb tunnel junctions with extremely low resistivity," *Electron. Lett*, vol. 42, no. 7, pp. 419–420, 2006.

[23] O. Dier, C. Reindl, A. Bachmann, C. Lauer, T. Lim, K. Kashani-Shirazi, and M.-C. Amann, "Reduction of hetero-interface resistivity in n-type AlAsSb/GaSb distributed Bragg reflectors," *Semicond. Sci. Technol.*, vol. 23, no. 2, pp. 025018-1–025018-4, 2008.

[24] O. Dier, S. Dachs, M. Grau, C. Lin, C. Lauer, and M.-C. Amann, "Effects of thermal annealing on the band gap of GaInAsSb," *Appl. Phys. Lett.*, vol. 86, pp. 151120-1–151120-3, 2005.

[25] K. Kashani-Shirazi, A. Bachmann, and M.-C. Amann, "Simulation of active regions for GaSb-based VCSELs," in *Proc. Nano-Optoelectron. Workshop (i-NOW 2008)*, pp. 137–138.

Alexander Bachmann (S'07) received the Diploma degree in physics from the Technische Universität München, Garching, Germany, in 2006. He is currently working toward the Ph.D. degree.

He is currently engaged in research on long-wavelength GaSb-based vertical-cavity surface-emitting lasers. He has authored or coauthored 13 papers in leading technical journals and conferences.

Kaveh Kashani-Shirazi received the Diploma degree in mechanical engineering from the Technische Universität München, Garching, Germany, in 1997. He is currently working toward the Ph.D. degree in electrical engineering at the Walter Schottky Institut, Technische Universität München.

He was with Voxeljet Technology GmbH, Augsburg, Germany. He has authored or coauthored seven papers in leading technical journals and conferences. His current research interests include the area of molecular beam epitaxy (MBE)-growth of antimonides for GaSb-based vertical-cavity surface-emitting laser.

Shamsul Arafin received the B.Sc. degree in electrical and electronics engineering from Bangladesh University of Engineering and Technology, Dhaka, Bangladesh, in 2005, and the M.Sc. degree in communication technology from Universität Ulm, Ulm, Germany, in 2008. He is currently working toward the Ph.D. degree at the Walter Schottky Institut, Garching, Germany.

His current research interests include GaSb-based vertical-cavity surface-emitting lasers (VCSELs) for wavelengths above 2 μm.

Markus-Christian Amann (A'88–SM'91–F'07) was born in Singen/Hohentwiel, Germany, in 1950. He received the Diploma degree in electrical engineering and the Dr.-Ing. degree from the Technical University of Munich, Munich, Germany, in 1976 and 1981, respectively.

During his thesis work, he studied superluminescent diodes and low-threshold laser diodes and developed the AlGaAs-GaAs metal-clad ridge-waveguide laser. From 1981 to 1994, he was with the Corporate Research Laboratories of the Siemens AG in Munich, where he was engaged in research on long-wavelength InGaAsP-InP laser diodes. In 1990, he became a Deputy Director for the research on laser diodes and integrated optoelectronic devices. On February 1994, he joined the Department of Electrical Engineering at the University of Kassel as a Full professor for "Technical Electronics" establishing a working group for III/V semiconductor electronics and optoelectronics. Since November 1997, he holds the Chair of Semiconductor Technology at the Walter Schottky Institute, Technical University of Munich, where he is currently engaged in research on tunable laser diodes for the near-IR, quantum cascade lasers, long-wavelength vertical-cavity laser diodes, and laser diode applications. He has authored or coauthored some 400 articles and talks (including some 50 invited) on semiconductor optoelectronics in scientific journals, conference proceedings. He has coauthored two books.

Prof. Amann is a member of the German Informationstechnische Gesellschaft (ITG), and a Fellow of the IEEE Lasers and Electro-Optics Society. He has served on numerous conference committees such as the IEEE Semiconductor Laser Conferences, the Indium Phosphide and Related Materials Conferences, and the Conferences on Lasers and Electro-Optics.